Received: 28 April 2020 | Revised: 31 July 2020 | Accepted: 24 August 2020

DOI: 10.4218/etrij.2020-0185

SPECIAL ISSUE

ETRI Journal WILEY

Performance analysis of satellite and terrestrial spectrum-shared networks with directional antenna

Jeong Seon Yeom[1] | **Gosan Noh**[2] | **Heesang Chung**[2] | **Ilgyu Kim**[2] | **Bang Chul Jung**[1]

[1]Department of Electronics Engineering, Chungnam National University, Daejon, Rep. of Korea

[2]Future Mobile Communication Research Division, Electronics and Telecommunications Research Institute, Daejon, Rep. of Korea

Correspondence
Bang Chul Jung, Department of Electronics Engineering, Chungnam National University, Daejon, Rep. of Korea.
Email: bcjung@cnu.ac.kr

Funding information
The research leading to these results received funding from the European Union H2020 under Grant No. 815323 and is supported by the Institute for Information & Communications Technology Promotion (IITP) grant funded by the Korean government (MSIT) (No. 2018-0-00175, 5G AgiLe and fLexible integration of SaTellite And cellulaR).

Abstract

Recently, to make the best use of limited and precious spectrum resources, spectrum sharing between satellite and cellular networks has received much interest. In this study, we mathematically analyze the success probability of a fixed (satellite) earth station (FES) based on a *stochastic geometry* framework. Both the FES and base stations (BSs) are assumed to be equipped with a directional antenna, and the location and the number of BSs are modeled based on the Poisson point process. Furthermore, an *exclusion zone* is considered, in which the BSs are prohibited from locating in a circular zone with a certain radius around the FES to protect it from severe interference from the cellular BSs. We validate the analytical results on the success probability of the *cognitive* satellite-terrestrial network with directional antennas by comparing it using extensive computer simulations and show the effect of the exclusion zone on the success probability at the FES. It is shown that the exclusion zone-based interference mitigation technique significantly improves the success probability as the exclusion zone increases.

KEYWORDS

cognitive satellite-terrestrial network, poisson point process, spectrum sharing, stochastic geometry, success probability

1 | INTRODUCTION

One of the most natural methods to meet beyond fifth-generation (B5G) system requirements, such as ultra-high data rates, ultra-low power consumption, intelligent network operation, and all-time seamless coverage, is to expand the utilized frequency bandwidth of wireless systems [1,2]. However, bandwidth expansion is not easy because of the scarcity of frequency resources. In addition, integrated satellite-terrestrial networks have received much attention from both industry and academia because satellites are expected to play an important role in the future B5G system to satisfy the requirements of ultra-high data rate and seamless coverage [3].

Recently, the Federal Communications Commission reallocated the 3.7 Ghz−4.5 GHz band (C-band), where the fixed (satellite) earth stations (FESs) are primarily incumbent for flexible use, including fifth-generation (5G) [4]. Within this band, the lower 280 MHz (3.7 GHz−3.98 GHz band) is allocated for mobile use and the next 20 MHz above (3.98 GHz−4.0 GHz) will serve as a guard band. Another band (4.0 GHz−4.2 GHz) will be provided to operate satellite networks with FES. Although there is a guard band, the existence of

different networks in adjacent channels may cause significant inter-network interference. In fact, the interference from 5G networks to satellite networks affects not only the C-band but also the 28 GHz bands, where only uplink fixed satellite services (FSSs) operate.

Therefore, interference mitigation/management techniques between fixed satellite networks and cellular networks have been actively investigated. In [5,6], the interference mitigation between the International Mobile Telecommunications-Advanced (IMT-A) and FSSs has been studied by exploiting a null-steering beamforming technique and protection zone concept, respectively. In the coexistence scenario of satellite up/downlinks and cellular downlinks, the required minimum protection radius around an FSS earth station according to the average aggregate interference threshold has been analyzed with omni-directional and directional base stations (BSs) [7]. In [8], interference mitigation techniques based on an angular-domain exclusion zone, uplink power control, and guard bands have been jointly investigated [8]. By considering a three-dimensional modeling map, the aggregate interference has been considered by computer simulations as well. In addition to these studies, [9–11] investigated the spectrum sharing and cognitive satellite-terrestrial network in which both satellite and terrestrial (including 5G) networks are downlinks. Among the existing interference mitigation techniques for FSSs, the separation between the FES and terrestrial stations with high output power has been particularly actively investigated in many studies. In this paper, we also include this separation as a baseline interference mitigation technique, and we call the protection region the *exclusion zone*.

The interference from each (terrestrial) cellular BS to the FSS in general depends on the distance between the BS and FSS as well as the beam orientation (boresight direction) of both stations with directional antennas. A stochastic geometry (SG) framework has been adopted to model geometric properties in analyzing the effect of interference in wireless networks [12–15]. In the SG framework, the Poisson point process (PPP) is typically utilized to model the locations of the transmitter. In [16], the outage probability of receivers (BSs and satellite users) was analyzed based on PPP in cognitive satellite-terrestrial networks that consist of stations with directional antennas. However, the closed-form outage probability was not provided, and only approximation was exploited to obtain the outage probability [16]. The characteristics of aggregate interference at a primary receiver in cognitive radio networks were analyzed in terms of the probability density function and cumulative distribution function, where the exclusion zone concept was adopted [17]. On the other hand, in [18], the effect of directional antenna on success probability, also known as coverage probability, was mathematically analyzed, but the exclusion zone was not considered.

In this study, we use the SG framework to mathematically analyze the success probability of the FES in a satellite and terrestrial spectrum-shared network where the cellular downlink is allowed to use the same frequency as that used by the satellite station (SS) downlink. We assume that all cellular BSs and the FES are equipped with directional antennas, and the locations of cellular BSs are modeled using a PPP. For tractability of mathematical analysis, the directional antennas have an ideal transmit/receive beam pattern, as in [18]. In particular, we consider the exclusion zone as an interference mitigation technique, in which cellular BSs are prohibited from deployment in a certain area around the FES. Through extensive computer simulations, the mathematical analysis is first validated and it is verified that the exclusion zone can efficiently improve the success probability.

Our contributions in this paper are summarized as follows:

1. For practical cellular networks, we consider the directional antenna gain in characterizing the interference from cellular to satellite networks.
2. The interference mitigation technique based on an exclusion zone is considered for the spectrum-shared network, and its performance is mathematically characterized.

The rest of this paper is organized as follows. In Section 2, the system model of the satellite and terrestrial spectrum-shared network with directional antennas and the concept of an exclusion zone are described. In Section 3, the success probability based on the SG is mathematically analyzed. Section 4 presents the numerical results and validates the mathematical analysis. Finally, the conclusions are drawn in Section 5.

2 | SYSTEM MODEL

We consider a spectrum-sharing scenario between a satellite and cellular networks, which consists of a single FES and multiple terrestrial BSs with directional antennas. We focus on the downlink case for both networks and thus only consider the interference from terrestrial cellular BSs to the FES. To protect the satellite communication from the interference of the cellular network, a circular exclusion zone is defined as the area where the BS of the cellular network cannot be deployed. The radius of the exclusion zone is assumed to be R_{E}.

The cellular network is modeled by a non-homogeneous PPP, $\Phi = \{x_k\}$, of intensity $\lambda > 0$ in the area outside the exclusion zone. The PPP Φ models the placement of the BS in two-dimensional ground, and then, $x_k \in \mathbb{R}^2$ represents the

location of the k-th BS. With the exclusion zone, a BS deployment constraint can be represented as $|x_i| > R_E$. Owing to Slivnyak's theorem [12], the FES is assumed to be located at the origin of a two-dimensional space (the ground). On the other hand, the SS that communicates with the FES is located in three-dimensional space at distance d_s and elevation angle θ_s from the FES. The distance d_s is calculated as $d_s\sqrt{6371^2\sin^2(\theta_s)+H_s^2+2\times H_s\times 6371}-6371\sin(\theta_s)$ (km) [19], where H_s denotes the altitude of the SS and 6371(km) is the Earth's radius.

2.1 | Gain patterns and orientation

The SS and FES are assumed to be equipped with the same three-dimensional directional antenna gain of G_s. The directional beam gain of certain direction at the FES is determined by two parameters: azimuth angle ϕ_s and elevation angle θ_s, that is, $G_s: \theta_s, \phi_s \to \mathbb{R}^+$ for a given beamwidth ω_s [18]. These two angles are relative angles based on the orientation of the FES. Without loss of generality, the orientation of the FES is assumed to have a negative value in the x-axis for a given elevation angle θ_s, as shown in Figure 1. On the other hand, the antenna gain pattern of BS G_c is dealt with in two-dimensional space on the ground because the height of the BSs is negligible compared with the SS and its beam direction faces down in general. Thus, G_c depends on the relative azimuth angle about the orientation of the BS ϕ_c, that is, $G_c: \phi_c \to \mathbb{R}^+$ for a given beamwidth ω_c.

For simplicity, we assume that the antenna gains of all stations have an ideal antenna beam pattern, as shown in Figure 2. The antenna beam patterns G_c and G_s are symmetric for an orientation angle. Specifically, beam pattern gain G_c has only two discrete values according to the side lobe and main lobe. Therefore, the probability mass function of G_c is given as follows:

$$p_{G_c}(g_c)=\begin{cases}\dfrac{\omega_c}{2\pi}, & \text{if } g_c=g_{c,1}\\ 1-\dfrac{\omega_c}{2\pi}, & \text{if } g_c=g_{c,2}\end{cases}, \tag{1}$$

where $g_{c,1}$ and $g_{c,2}$ denote the gains of the main and side lobes of the BSs, respectively, and the beam gain of the BSs is normalized for all directions, that is, $(1/2\pi)\int_{-\pi}^{\pi} G_c(\theta)\,d\theta = 1$. Thus, the gain of the main lobes of the BSs is obtained for a given $g_{c,2}$ $(0 < g_{c,2} < 2\pi/(2\pi-\omega_c))$ as

$$g_{c,1}=\frac{2\pi-g_{c,2}(2\pi-\omega_c)}{\omega_c}>0. \tag{2}$$

For beam pattern gain $G_{s|\theta_s}$, if the elevation angles of FES θ_s are greater than $\omega_s/2$, the beam pattern gain has a single gain value in the side lobe in the direction of the BSs. However, if θ_s is smaller than $\omega_s/2$, the beam pattern gain has two discrete gain values according to the side lobe and main lobe for the direction to the BSs.

$$p_{G_{s|\theta_s}}(g_s)=\begin{cases}\dfrac{\omega_s}{2\pi}, & \text{if } g_s=g_{s,1}\\ 1-\dfrac{\omega_s}{2\pi}, & \text{if } g_s=g_{s,2}\end{cases}, \text{ for } 0\le\theta_s\le\frac{\omega_s}{2}, \tag{3}$$

$$p_{G_{s|\theta_s}}(g_s)=1, \text{ if } g_s=g_{s,2}, \text{ for } \frac{\omega_s}{2}\le\theta_s\le\frac{\pi}{2}, \tag{4}$$

where $g_{s,1}$ and $g_{s,2}$ denote the gains of the main and side lobes of stations in the satellite network, respectively. In addition, for the normalized beam gain, $g_{s,1}$ and $g_{s,2}$ are given as follows:

$$g_{s,2}=\frac{P_{t,s}}{A_2(\omega_s)}, \quad g_{s,1}=\frac{4\pi-g_{s,2}(A-A_2(\omega_s))}{(A-A_2(\omega_s))}, \tag{5}$$

where $A = 4\pi$, $A_1(\omega_s)=\int_{\theta=0}^{\omega_s}\int_{\phi=0}^{\omega_s}\sin(\phi)\,d\phi d\theta$, $A_2(\omega_c) = A - A_1(\omega_c)$, and $P_{t,s}$ denotes the transmit power at the SS.

Figure 3 shows an example of the network model where the exclusion zone is applied in the satellite and cellular coexistence network. The blue asterisk at the origin represents the FES, and the black, blue, magenta, and red circles represent the randomly distributed cellular BSs that have the side lobe-to-side lobe, main lobe-to-side lobe, side lobe-to-main lobe, and main lobe-to-main lobe

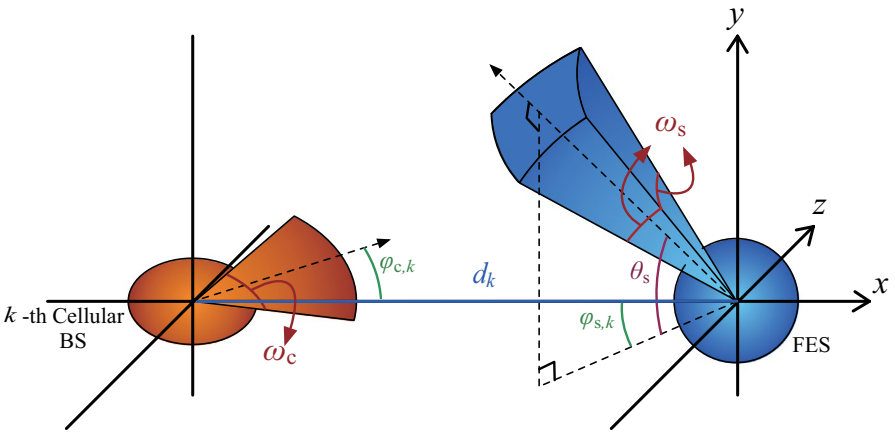

FIGURE 1 System model on the ground where the cellular BSs and the FES exist.

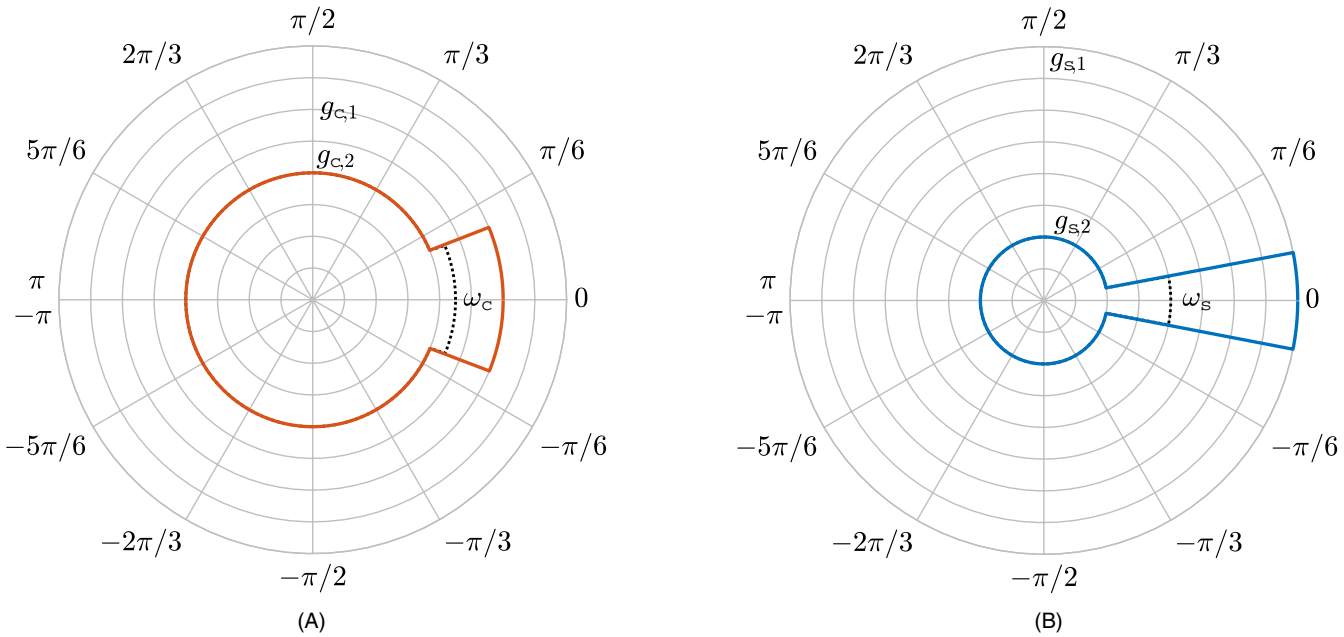

FIGURE 2 Ideally symmetric and sectorized beam pattern of stations: (A) Cellular BS, G_c and (B) Stations in satellite network, G_s.

TX-RX beam patterns, respectively. The circular sector radiated at each point represents the main lobe beam. The red translucent circle around the origin represents the exclusion zone.

2.2 | Channel model

In this paper, we consider large-scale propagation loss with small-scale Rayleigh fading when modeling the channel between stations. The received interference power at the FES from the k-th BS is given by

$$P_{r,k} = P_{t,c} G_c\left(\phi_{c,k}\right) G_s\left(\theta_s, \phi_{s,k}\right) h_k d_k^{-\alpha_1}, \tag{6}$$

where $P_{t,c}$ denotes the transmit power of the BSs, $\phi_{c,k}$ denotes the relative azimuth angle of the FES from the orientation angle of the k-th BS, and $\phi_{s,k}$ denotes the relative azimuth angle of the k-th BS from the orientation angle of the FES. Both angles $\phi_{c,k}$ and $\phi_{s,k}$ become uniformly distributed over $[-\pi, \pi)$. The distance between the k-th BS and the FES is represented as $d_k(:=\|x_k\|)$, and α_1 denotes the path-loss exponent of the wireless link between a BS and the FES. We assume $\alpha_1 = 3$ in this study. The small-scale fading channel gain from the k-th BS to FES h_k is assumed to follow an identically independently distributed exponential distribution, that is, h_k:-exp(1). Similarly, the received signal power at the FES from the SS is given by

$$P_{r,s} = P_{t,s} g_{c,1} g_{c,1} h_s L(d_s, \theta_s, f_c)^{-1}, \tag{7}$$

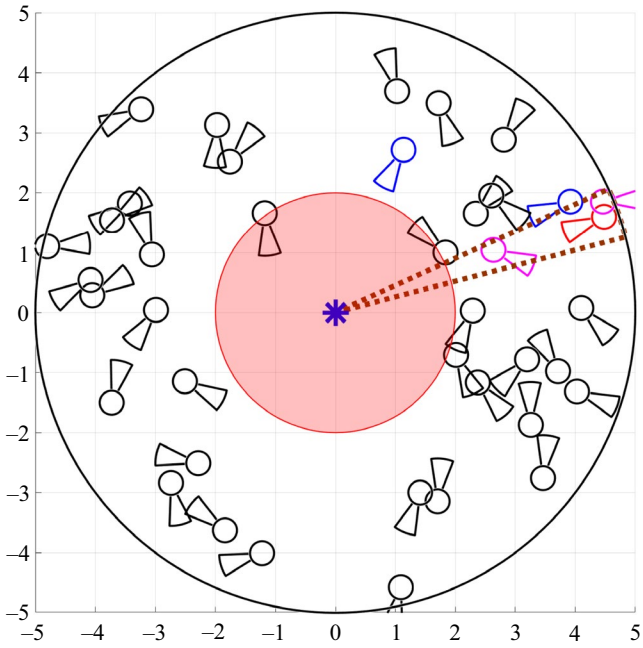

FIGURE 3 Exclusion zone-based network model with directional antenna nodes.

where h_s denotes the fading channel gain of the satellite signal link, which is also assumed to follow an exponential distribution with unit mean. Further, $L(d_s, \theta_s, f_c)$ denotes a simplified path loss, referring to the path loss provided by 3GPP and ITU-R in a non-terrestrial network [19,20]. Under the assumptions of an

open environment for the FES, line of sight, and no scintillation, the path loss in dB is given as follows:

$$L\left(d_{\mathrm{s}},\theta_{\mathrm{s}},f_{\mathrm{c}}\right)=32.45+20\log_{10}\left(f_{\mathrm{c}}\right)+20\log_{10}\left(d_{\mathrm{s}}\right)+\frac{4\times10^{-2}}{\sin\left(\theta_{\mathrm{s}}\right)}, \quad (8)$$

where f_{c} denotes the center frequency in Ghz and is given as four in this study. We assume the orientations of the SS and FES are perfectly steered toward each other, that is, a satellite signal is sent and received via a main lobe-to-main lobe antenna beam pattern.

At the FES, the success probability of communication is defined as

$$\mathscr{P}_{\mathrm{S}}=\Pr\{\mathrm{SINR}\geq\beta\}=Pr\left\{\frac{P_{\mathrm{r,s}}}{\sum_{k=1}^{K}P_{\mathrm{r},k}+N_0}\geq\beta\right\}, \quad (9)$$

where N_0 denotes the thermal noise power at the FES and β denotes the signal-to-interference-plus-noise ratio (SINR) threshold for the success probability.

3 | PERFORMANCE ANALYSIS OF THE SUCCESS PROBABILITY

In this section, we mathematically analyze the success probability of FES in the coexistence of FSS and cellular network with the exclusion zone, where BSs are distributed based on the PPP. The success probability (9) is given as a tractable form as follows:

$$\begin{aligned}\mathscr{P}_{\mathrm{S}}&=\Pr\left\{\frac{P_{\mathrm{r,s}}}{\sum_{k=1}^{K}P_{\mathrm{r},k}+N_0}\geq\beta\right\}\\&=\Pr\left\{\frac{P_{\mathrm{t,s}}g_{\mathrm{s},1}^2h_{\mathrm{s}}L(d_{\mathrm{s}},\theta_{\mathrm{s}},f_{\mathrm{c}})^{-1}}{\sum_{k=1}^{K}P_{\mathrm{t,c}}G_{\mathrm{c}}(\phi_{\mathrm{c},k})G_{\mathrm{s}}(\theta_{\mathrm{s}},\phi_{\mathrm{s},k})h_kd_k^{-\alpha_I}+N_0}\geq\beta\right\}\\&\overset{(a)}{=}\Pr\left\{h_{\mathrm{s}}\geq\frac{\beta\sum_{k=1}^{K}P_{\mathrm{t,c}}G_c(\phi_{\mathrm{c},k})G_{\mathrm{s}}(\theta_{\mathrm{s}},\phi_{\mathrm{s},k})h_kd_k^{-\alpha_I}}{P_{\mathrm{t,s}}g_{\mathrm{s},1}^2L(d_{\mathrm{s}},\theta_{\mathrm{s}},f_{\mathrm{c}})^{-1}}\right\}\\&\quad\times\Pr\left\{P_{\mathrm{t,s}}\geq\frac{\beta N_0}{g_{\mathrm{s},1}^2h_{\mathrm{s}}L(d_{\mathrm{s}},\theta_{\mathrm{s}},f_{\mathrm{c}})^{-1}}\right\}\\&=\mathbb{E}_{I_0}\left[\exp\left(-sI_0\right)\right]\exp\left(-sN_0\right),\end{aligned} \quad (10)$$

where (a) comes from the memoryless property of exponential distribution, $I_0=\sum_{k=1}^{K}P_{\mathrm{t,c}}G_{\mathrm{c}}\left(\phi_{\mathrm{c},k}\right)G_{\mathrm{s}}\left(\theta_{\mathrm{s}},\phi_{\mathrm{s},k}\right)h_kd_k^{-\alpha_I}$ and $s=\beta/(P_{\mathrm{t,s}}g_{\mathrm{s},1}^2L(d_{\mathrm{s}},\theta_{\mathrm{s}},f_{\mathrm{c}})^{-1})$.

In (10), the first expectation can be expressed as

$$\begin{aligned}\mathbb{E}_{I_0}\left[\exp\left(-sI_0\right)\right]&=\mathbb{E}_{\Phi,G_{\mathrm{c}},G_{\mathrm{s}},h_k}\left[\prod_{x_k\in\Phi}e^{-sP_{\mathrm{t,c}}G_{\mathrm{c}}(\phi_{\mathrm{c},k})G_{\mathrm{s}}(\theta_{\mathrm{s}},\phi_{\mathrm{s},k})h_kd_k^{-\alpha_I}}\right]\\&=\mathbb{E}_{\Phi}\left[\prod_{x_k\in\Phi}\mathbb{E}_{G_{\mathrm{c}},G_{\mathrm{s}|\theta_{\mathrm{s}}},h}\left[e^{-sP_{\mathrm{t,c}}G_{\mathrm{c}}G_{\mathrm{s}|\theta_{\mathrm{s}}}hd_k^{-\alpha_I}}\right]\right]\\&=\mathbb{E}_{\Phi}\left[\prod_{x_k\in\Phi}v\left(||x_k||\right)\right]\overset{(b)}{=}\exp\left[-\int_{R_{\mathrm{E}}}^{\infty}\left\{1-v\left(x\right)\right\}\lambda(x)dx\right]\\&=\exp\left[-\int_{R_{\mathrm{E}}}^{\infty}\mathbb{E}_{G_{\mathrm{c}},G_{\mathrm{s}|\theta_{\mathrm{s}}},h}\left[1-e^{-sP_{\mathrm{t,c}}G_{\mathrm{c}}G_{\mathrm{s}|\theta_{\mathrm{s}}}hx^{-\alpha_I}}\right]\lambda(x)dx\right],\end{aligned} \quad (11)$$

where (b) comes from Campbell's theorem and considers that the intensity on the exclusion zone is equal to zero, that is, $\lambda(x)=0$ for $0\leq x\leq R_{\mathrm{E}}$.

In (11), the integration is solved as

$$\begin{aligned}&\int_{R_{\mathrm{E}}}^{\infty}\mathbb{E}_{G_{\mathrm{c}},G_{\mathrm{s}|\theta_{\mathrm{s}}},h}\left[1-e^{-sP_{\mathrm{t,c}}G_{\mathrm{c}}G_{\mathrm{s}|\theta_{\mathrm{s}}}hx^{-\alpha_I}}\right]\lambda\left(x\right)dx\\&=\mathbb{E}_{G_{\mathrm{c}},G_{\mathrm{s}|\theta_{\mathrm{s}}},h}\left[\lambda\pi\int_{R_{\mathrm{E}}}^{\infty}\left(1-e^{-sP_{\mathrm{t,c}}G_{\mathrm{c}},G_{\mathrm{s}|\theta_{\mathrm{s}}}hx^{-\alpha_I}}\right)2xdx\right]\\&=\lambda\pi\mathbb{E}_{G_{\mathrm{c}},G_{\mathrm{s}|\theta_{\mathrm{s}}},h}\left[\left\{\left(1-e^{-\rho hR_{\mathrm{E}}^{-\alpha_I}}\right)\left(-R_{\mathrm{E}}^2\right)+(\rho h)^{\frac{2}{\alpha_I}}\right.\right.\\&\qquad\left.\left.\times\gamma\left(1-\frac{2}{\alpha_I},\rho hR_{\mathrm{E}}^{-\alpha_I}\right)\right\}\right],\end{aligned} \quad (12)$$

where $\rho:=sP_{\mathrm{t,c}}G_{\mathrm{c}}G_{\mathrm{s}|\theta_{\mathrm{s}}}$ and $\gamma(\cdot)$ is the lower incomplete gamma function. We calculate the expectation for h in (12) as

$$\begin{aligned}&\mathbb{E}_h\left[\left\{\left(1-e^{-\rho hR_{\mathrm{E}}^{-\alpha_I}}\right)\left(-R_{\mathrm{E}}^2\right)+(\rho h)^{\frac{2}{\alpha_I}}\gamma\left(1-\frac{2}{\alpha_I},\rho hR_{\mathrm{E}}^{-\alpha_I}\right)\right\}\right]\\&=\int_0^{\infty}\left(1-e^{-\rho hR_{\mathrm{E}}^{-\alpha_I}}\right)\left(-R_E^2\right)e^{-h}dh\\&\quad+\int_0^{\infty}(\rho h)^{\frac{2}{\alpha_I}}\gamma\left(1-\frac{2}{\alpha_I},\rho hR_{\mathrm{E}}^{-\alpha_I}\right)e^{-h}dh.\end{aligned} \quad (13)$$

In (13), the integration of the first term is solved as and the second term is given as

$$\begin{aligned}&\int_0^{\infty}\left(1-e^{-\rho hR_{\mathrm{E}}^{-\alpha I}}\right)\left(-R_E^2\right)e^{-h}dh\\&=\left(-R_{\mathrm{E}}^2\right)\int_0^{\infty},\left(e^{-h}-e^{-\left(\rho R_{\mathrm{E}}^{-\alpha_I}+1\right)h}\right)dh=-\frac{\rho R_{\mathrm{E}}^{2-\alpha_I}}{\rho R_{\mathrm{E}}^{-\alpha_I}+1},\end{aligned} \quad (14)$$

$$\begin{aligned}&\int_0^{\infty}(\rho h)^{\frac{2}{\alpha_I}}\gamma\left(1-\frac{2}{\alpha_I},\rho hR_{\mathrm{E}}^{-\alpha_I}\right)e^{-h}dh\\&=\rho^{\frac{2}{\alpha_I}}\int_0^{\infty}h^{\left(1+\frac{2}{\alpha_I}\right)-1}e^{-h}\gamma\left(1-\frac{2}{\alpha_I},\rho hR_{\mathrm{E}}^{-\alpha_I}\right)dh\\&=\frac{\rho R_{\mathrm{E}}^{2-\alpha_I}}{\left(1-\frac{2}{\alpha_I}\right)\left(\rho R_{\mathrm{E}}^{-\alpha_I}+1\right)^2}\,{}_2F_1\left(1,2;2-\frac{2}{\alpha_I};\frac{\rho R_{\mathrm{E}}^{-\alpha_I}}{\rho R_{\mathrm{E}}^{-\alpha_I}+1}\right),\end{aligned} \quad (15)$$

$$\lambda\pi\mathbb{E}_{G_c,G_{s|\theta_s}}\left[-\frac{\rho R_E^{2-\alpha_I}}{\rho R_E^{-\alpha_I}+1}+\frac{\rho R_E^{2-\alpha_I}}{\left(1-\frac{2}{\alpha_I}\right)\left(\rho R_E^{-\alpha_I}+1\right)^2}\,{}_2F_1\left(1,2;2-\frac{2}{\alpha_I};\frac{\rho R_E^{-\alpha_I}}{\rho R_E^{-\alpha_I}+1}\right)\right] \tag{16}$$

$$=\lambda\pi\int_0^\infty\int_0^\infty\left\{-\frac{\rho R_E^{2-\alpha_I}}{\rho R_E^{-\alpha_I}+1}+\frac{\rho R_E^{2-\alpha_I}}{\left(1-\frac{2}{\alpha_I}\right)\left(\rho R_E^{-\alpha_I}+1\right)^2}\,{}_2F_1\left(1,2;2-\frac{2}{\alpha_I};\frac{\rho R_E^{-\alpha_I}}{\rho R_E^{-\alpha_I}+1}\right)\right\}p_{G_c}(g_c)\,p_{G_{s|\theta_s}}(g_s)\,dg_c dg_s$$

$$=\lambda\pi\sum_{g_c\in\{g_{c,1},g_{c,2}\}}\sum_{g_s\in\{g_{s,1},g_{s,2}\}}\left\{-\frac{sP_{t,c}g_cg_sR_E^{2-\alpha_I}}{sP_{t,c}g_cg_sR_E^{-\alpha_I}+1}+\frac{sP_{t,c}g_cg_sR_E^{2-\alpha_I}}{\left(1-\frac{2}{\alpha_I}\right)\left(sP_{t,c}g_cg_sR_E^{-\alpha_I}+1\right)^2}\,{}_2F_1\left(1,2;2-\frac{2}{\alpha_I};\frac{sP_{t,c}g_cg_sR_E^{-\alpha_I}}{sP_{t,c}g_cg_sR_E^{-\alpha_I}+1}\right)\right\}p_{G_c}(g_c)\,p_{G_s}(g_s).$$

$$\mathcal{P}_S=\exp\left[sN_0-\lambda\pi\sum_{g_c\in\{g_{c,1},g_{c,2}\}}\sum_{g_s\in\{g_{s,1},g_{s,2}\}}\left\{\frac{sP_{t,c}g_cg_sR_E^{2-\alpha_I}}{sP_{t,c}g_cg_sR_E^{-\alpha_I}+1}+\frac{sP_{t,c}g_cg_sR_E^{2-\alpha_I}}{\left(1-\frac{2}{\alpha_I}\right)\left(sP_{t,c}g_cg_sR_E^{-\alpha_I}+1\right)^2}\,{}_2F_1\left(1,2;2-\frac{2}{\alpha_I};\frac{sP_{t,c}g_cg_sR_E^{-\alpha_I}}{sP_{t,c}g_cg_sR_E^{-\alpha_I}+1}\right)\right\}p_{G_c}(g_c)\,p_{G_s}(g_s)\right]. \tag{17}$$

where ${}_2F_1$ is a Gaussian hypergeometric function. Substituting (14) and (15) into (12) and taking the expectation of the beam gains, (16) is given by including the probability mass function of beam patterns p_{G_c} and p_{G_s}. Finally, the success probability at the FES where the satellite and cellular networks coexist is derived as (17).

4 | SIMULATION RESULTS

In this section, we validate the mathematical analysis in Section 3 through extensive Monte Carlo simulations. The simulation parameters are summarized in Table 1.

Figure 4 shows the success probability of the FES for varying values of density (λ) of the cellular BS in the satellite and terrestrial spectrum-shared network with directional antennas. In particular, various SINR threshold values β and two distinct altitude angles of the FES θ_s are considered for a given $R_E = 2000$ m. It is worth noting that the analytical results match well with the simulation results, which validates the mathematical analysis proposed in this paper. As the SINR threshold increases or the density of the BSs increases, the success probability decreases for all θ_s, as expected. For case 2, the interference from BSs becomes relatively large because $\omega_s/2 > \theta_s$. Then, the success probability decreases quickly as the density of the BSs increases in this case. For case 1, on the other hand, the interference from the BSs becomes relatively small because $\omega_s/2 < \theta_s$. In this case, the success probability decreases slowly as the density of BSs increases because all interference from the BSs arrives at the FES via a side-lobe antenna beam pattern.

TABLE 1 Simulation parameters

Parameter	Value
$P_{t,s}$	20 W
$P_{t,c}$	10 W
H_s	600 km
α_I	3
ω_s	7°
ω_c	30°
$g_{s,1}$	41.40 dBi
$g_{s,2}$	−10 dBi
$g_{c,1}$	10 dBi
$g_{c,2}$	−7.40 dBi
Bandwidth	10 MHz
Noise spectral density	−172.6 dBm/Hz

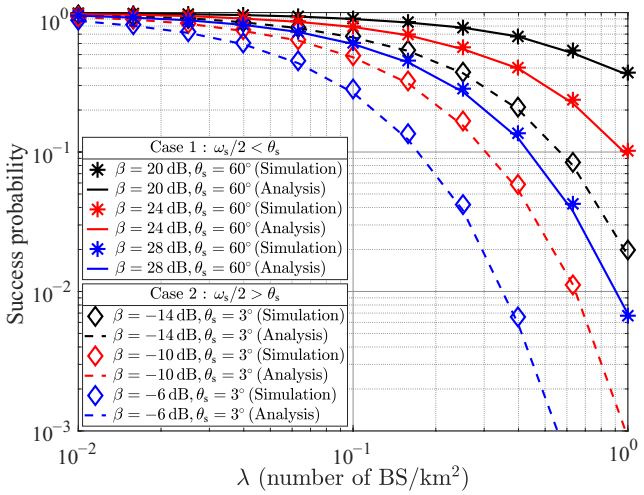

FIGURE 4 Success probability of FES when varying the density of terrestrial BSs.

Figure 5 shows the success probability of the FES for various radius values of the exclusion zone R_E when $\lambda = 1$ is the number of BSs/km^2. The results for various θ_s and β values are similar to the results in Figure 4. When R_E is same as 0, the SINR thresholds β of cases 1 and 2 are set, and the

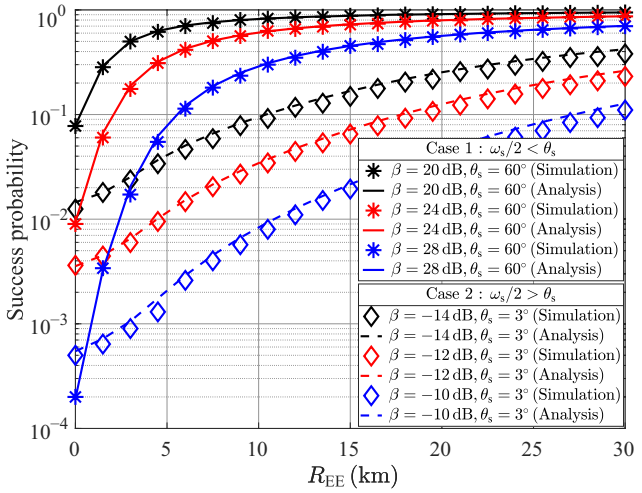

FIGURE 5 Success probability of FES for various exclusion zone radius values, R_E.

simulation results with the same color line do not differ significantly. As R_E increases, case 1 appears more rapidly than case 2 in terms of the change in performance of success probability. This means that R_E is much more dominant in case 1 than in case 2. This is because the power of the satellite signal received at the FES is stronger in case 1 than in case 2 because of the path loss and the distance between the SS and FES. Another reason is that the larger average interference temperature reduces the dependent influence on the distance to the interferers.

In Figure 6, the simulation results show the success probability of FES for various FES elevation angles, θ_s, which

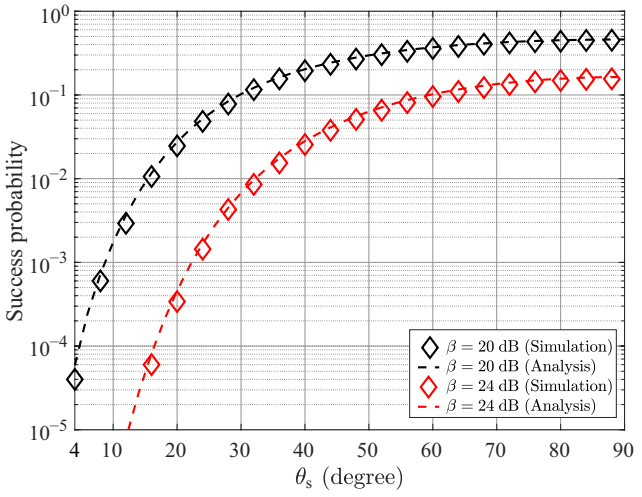

FIGURE 6 Success probability of FES for various elevation angles of the FES, θ_s.

is greater than $\omega_s/2$, with various thresholds when $\lambda = 1$ is the number of BSs/km^2. As the elevation angle increases, the distance between the SS and FES is smaller and the effect of atmospheric gases in the path loss term is reduced, which increases the performance. According to θ_s, the rate of change of success probability in the dB domain is different because all θ_s in the path loss vary as a sine function and for low θ_s, the amount of change in the sine function is relatively large compared to that of θ_s.

In Figures 5 and 6, we can see that our mathematical analysis has significant value by comparing the analytical and simulation results.

5 | CONCLUSIONS

In this study, the performance of a satellite and terrestrial spectrum-shared network with directional antennas was mathematically analyzed based on an SG framework. In particular, the success probability of an FES was investigated by considering the interference from multiple BSs. An ideal directional antenna beam pattern was assumed for mathematical tractability, and a circular exclusion zone was considered as an interference mitigation technique. Through computer simulations, the analytical results proposed in this paper were validated for various system parameters.

ACKNOWLEDGMENTS

The research leading to these results received funding from the European Union H2020 under Grant No. 815323 and is supported by the Institute for Information & Communications Technology Promotion (IITP) grant funded by the Korean government (MSIT) (No. 2018-0-00175, 5G AgiLe and fLexible integration of SaTellite And cellulaR).

CONFLICT OF INTEREST

The authors declare no potential conflicts of interest.

AUTHOR CONTRIBUTIONS

Jeong Seon Yeom performed the computer simulations and wrote the original draft. Gosan Noh, Heesang Chung, and Ilgyu Kim surveyed the literature and helped write the paper. Bang Chul Jung designed the research study, performed the mathematical analysis, and helped write the paper.

ORCID

Jeong Seon Yeom https://orcid.org/0000-0003-0480-034X
Bang Chul Jung https://orcid.org/0000-0002-4485-9592

REFERENCES

1. K. David and H. Berndt, *6G vision and requirements: Is there any need for beyond 5G?*, IEEE Veh. Technol. Mag. **13** (2018), 72–80.
2. Z. Zhang et al., *6G wireless networks: Vision, requirements, architecture, and key technologies*, IEEE Veh. Technol. Mag. **14** (2019), 28–41.
3. M. Jia et al., *Intelligent resource management for satellite and terrestrial spectrum shared networking toward B5G*, IEEE Wirel. Commun. **27** (2020), 54–61.
4. The Federal Communications Commission, In the matter of expanding flexible use of the 3.7 to 4.2 GHz band, Report and Order FCC 20–22, 2020.
5. J.-W. Lim et al., *Interference mitigation technique for the sharing between IMT-Advanced and fixed satellite service*, J. Commun. Networks **9** (2007), 159–166.
6. S. Aijaz, *Effects of deploying IMT-Advanced systems on fixed satellite services in the 3,400–3,600 MHZ frequency band in Pakistan*, in Proc. Int. Conf. Adv. Space Technol. (Islamabad, Pakistan), 2008, https://doi.org/10.1109/ICAST.2008.4747676
7. C. Zhang et al., *Spatial spectrum sharing for satellite and terrestrial communication networks*, IEEE Trans. Aerosp. Electron Syst. **55** (2019), 1075–1089.
8. G. Hattab et al., *Interference analysis of the coexistence of 5G cellular networks with satellite earth stations in 3.7-4.2GHz*, in Proc. IEEE Int. Conf. Commun. Workshops (Kansas City, MO, USA), 2018. https://doi.org/10.1109/ICCW.2018.8403528
9. S. Kim et al., *Coexistence of 5G with the incumbents in the 28 and 70 GHz bands*, IEEE J. Sel. Areas Commun. **35** (2017), 1254–1268.
10. M. Höyhtyä et al., *Database-assisted spectrum sharing in satellite communications: A survey*, IEEE Access. **5** (2017), 25322–25341.
11. Q. Zhang et al., *Coexistence and performance limits for the cognitive broadband satellite system and mmWave cellular network*, IEEE Access. **8** (2020), 51905–51917.
12. M. Haenggi, Stochastic geometry for wireless networks, Cambridge Univ, Cambridge, UK, 2013.
13. H. Jin et al., *Energy efficiency of ultra-dense small-cell networks with adaptive cell-breathing*, IET Commun. **12** (2018), 367–372.
14. W. Lee, B. C. Jung, and H. Lee, *ACEnet: Approximate thinning based judicious network control for energy-efficient ultra-dense networks*, MDPI Energies **11** (2018), no. 5.1307.
15. E. Chu, J. M. Kim, and B. C. Jung, *Interference modeling and analysis in 3-dimensional directional UAV networks based on stochastic geometry*, Elsevier ICT Express **5** (2019), 235–239.
16. O. Y. Kolawole et al., *On the performance of cognitive satellite-terrestrial networks*, IEEE Trans. Cognit. Commun. Network. **3** (2017), no. 4, 668–683.
17. Z. Chen et al., *Aggregate interference modeling in cognitive radio networks with power and contention control*, IEEE Trans. Commun. **60** (2012), 456–468.
18. J. Wildman et al., *On the joint impact of beamwidth and orientation error on throughput in directional wireless poisson networks*, IEEE Trans. Wireless Commun. **13** (2014), 7072–7085.
19. The 3rd Generation Partnership Project (3GPP), *Study on New Radio (NR) to support non-terrestrial networks (Release 15)*, Tech. Report 38.811 v15.2.0, Sep. 2019.
20. International Telecommunication Union (ITU), *Attenuation by atmospheric gases*, *Recommendation ITU-R P.676-11*, September 2016.

AUTHOR BIOGRAPHIES

Jeong Seon Yeom received his BS degree in electronics engineering and MS degree in electronics, radio sciences, and engineering and information communications engineering from Chungnam National University, Daejeon, Rep. of Korea in 2017 and 2019, respectively. He is currently a PhD student studying communications and signal processing in electronics engineering at Chungnam National University, Daejeon, Rep. of Korea. His research interests include non-orthogonal multiple access, multiple-input multiple-output, and interference mitigation in wireless communication systems.

Gosan Noh received his BS and PhD degrees in electrical and electronic engineering from Yonsei University, Seoul, Rep. of Korea, in 2007 and 2012, respectively. From March 2012 to February 2013, he was a postdoctoral researcher at the School of Electrical and Electronic Engineering, Yonsei University, Seoul, Rep. of Korea. Since March 2013, he has been with the Electronics and Telecommunications Research Institute (ETRI), Daejeon, Rep. of Korea, where he is a senior researcher. He has contributed to several areas of telecommunications including cognitive radio, spectrum sharing, millimeter-wave transmission, and high-mobility applications. He has published 45 scientific papers in journals and conferences. He has also been involved in 3rd Generation Partnership Project (3GPP) Fifth-Generation New Radio standardization as ETRI's delegate of the 3GPP RAN1 working group since 2016.

Heesang Chung received his BS degree in physics from Korea Advanced Institute of Science and Technology (KAIST), Daejeon, Rep. of Korea in 1993 and his PhD degree in physics from Chungnam National University, Daejeon, Rep. of Korea in 1999. Since 1999, he has been with the Electronics and Telecommunications Research Institute (ETRI), Daejeon, Rep. of Korea. He was involved in research projects on optical communications from 1999 to 2005. He moved to the Wireless Communications department of ETRI in 2005. He was involved in research projects on Long-Term Evolution (LTE) and LTE-Advanced from 2006 to 2010. His recent research interests are Fifth-Generation and millimeter-wave based mobile communications, including mobile wireless backhauls for public transportation.

Ilgyu Kim received his BS and MS degrees in electronics engineering from the University of Seoul, Seoul, Rep. of Korea, in 1993 and 1995, and his PhD degree in information communications engineering from Korea Advanced Institute of Science and Technology (KAIST), Daejeon, Rep. of Korea, in 2009. He worked for Shinsegi Telecoms from 1994 to 1999, where he took part in the optimization of the IS-95 Code-Division Multiple Access (CDMA) radio network and the international standardization of Wideband CDMA (WCDMA). Since 2000, he has been with the Electronics and Telecommunications Research Institute (ETRI), Daejeon, Rep. of Korea, where he was involved in the standardization and development of WCDMA, High Speed Packet Access, and Long-Term Evolution (LTE). He was in charge of the development of the LTE User Equipment modem chip set and Mobile Hotspot Network system. Since 2019, he has been the assistant vice president of ETRI and managing director of the Future Mobile Communication Research Division. Currently, his main research interests include millimeter-wave/THz communications and future mobile communications.

Bang Chul Jung received his BS degree in electronics engineering from Ajou University, Suwon, Rep. of Korea, in 2002, and his MS and PhD degrees in electrical and computer engineering from Korea Advanced Institute of Science and Technology (KAIST), Daejeon, Rep. of Korea, in 2004 and 2008, respectively. He was a senior researcher/research professor with the KAIST Institute for Information Technology Convergence, Daejeon, Rep. of Korea, from 2009 to 2010. From 2010 to 2015, he was a faculty member of Gyeongsang National University, Tongyeong, Rep. of Korea. He is currently a professor with the Department of Electronics Engineering, Chungnam National University, Daejeon, Rep. of Korea. His research interests include wireless communication systems, Internet-of-Things communications, statistical signal processing, information theory, interference management, radio resource management, spectrum sharing techniques, and machine learning.